THE JOURNAL OF BIOLOGICAL CHEMISTRY VOL. 285, NO. 51, pp. 40081–40087, December 17, 2010

Novel Channel Enzyme Fusion Proteins Confer Arsenate Resistance*[S]

Received for publication, September 13, 2010, and in revised form, October 12, 2010 Published, JBC Papers in Press, October 14, 2010, DOI 10.1074/jbc.M110.184457

Binghua Wu[1], **Jie Song**[1], **and Eric Beitz**[2]

From the Department of Pharmaceutical and Medicinal Chemistry, Christian-Albrechts-Universität zu Kiel, 24118 Kiel, Germany

Steady exposure to environmental arsenic has led to the evolution of vital cellular detoxification mechanisms. Under aerobic conditions, a two-step process appears most common among microorganisms involving reduction of predominant, oxidized arsenate ($H_2As^VO_4^-$/$HAs^VO_4^{2-}$) to arsenite ($As^{III}(OH)_3$) by a cytosolic enzyme (ArsC; *Escherichia coli* type arsenate reductase) and subsequent extrusion via ArsB (*E. coli* type arsenite transporter)/ACR3 (yeast type arsenite transporter). Here, we describe novel fusion proteins consisting of an aquaglyceroporin-derived arsenite channel with a C-terminal arsenate reductase domain of phosphotyrosine-phosphatase origin, providing transposable, single gene-encoded arsenate resistance. The fusion occurred in actinobacteria from soil, *Frankia alni*, and marine environments, *Salinispora tropica*; *Mycobacterium tuberculosis* encodes an analogous ACR3-ArsC fusion. Mutations rendered the aquaglyceroporin channel more polar resulting in lower glycerol permeability and enhanced arsenite selectivity. The arsenate reductase domain couples to thioredoxin and can complement arsenate-sensitive yeast strains. A second isoform with a nonfunctional channel may use the mycothiol/mycoredoxin cofactor pool. These channel enzymes constitute prototypes of a novel concept in metabolism in which a substrate is generated and compartmentalized by the same molecule. Immediate diffusion maintains the dynamic equilibrium and prevents toxic accumulation of metabolites in an energy-saving fashion.

Arsenic is widely present in nature (1). Its oxidation state is determined by the availability of oxygen and varies between −III, 0, III, and V. Reduced states of arsenic are found in anoxic environments and respective microorganisms have developed defense systems based on oxidation of As(III) (2). Since the advent of photosynthesis and a mostly aerobic environment on earth, arsenic predominates in the form of the inorganic oxyanion of As(V), *i.e.* arsenate (1). Arsenate chemically mimics phosphate and acts as a substitute in biochemical processes (3). As a result, arsenate is actively taken up via phosphate transporters and exerts acute toxicity by uncoupling ATP synthesis due to the formation of rapidly hydrolysable arsenyl-ADP (4). Cells convert arsenate to arsenite using small cytosolic ArsC reductases (5). Yet, arsenite is even more toxic because it forms stable covalent bonds with thiols blocking enzyme activity of *e.g.* pyruvate dehydrogenase (6) or thioredoxin reductase (7) and causing cancer in the long term (8). Therefore, rapid extrusion of arsenite from a cell is vital. Two unrelated families of unidirectional arsenite transporters have been identified in microorganisms, ArsB and ACR3 with 12 and 10 putative transmembrane spans, respectively (9). ArsB can associate with an ATPase subunit to enhance export rates. Recently, tetrameric aquaglyceroporin solute channels have been implicated in bidirectional arsenite transport (10, 11). Certain bacteria even lack genes for ArsB or ACR3 transporters and apparently release arsenite via an aquaglyceroporin (12). Here, we report on recent evolutional events fusing both, an arsenite transporting domain and an arsenate reductase domain, into a single unit. We describe ArsC fusion proteins with aquaglyceroporin-derived channel domains in actinobacteria from soil (*F. alni*, Ref. 13, Fraal3366) and marine environments (*S. tropica* (14) Strop634 and Strop1447; supplemental Fig. S1) and further show that a single *Mycobacterium tuberculosis* (15) gene, *Rv2643*, coding for a so far uncharacterized ACR3-ArsC fusion protein also confers arsenate resistance in a highly sensitive yeast strain.

EXPERIMENTAL PROCEDURES

Salinispora tropica Strain, Culture Conditions, and Isolation of Genomic DNA—S. tropica CNB-440 was obtained from the German Collection of Microorganisms and Cell Cultures (DSMZ) and was cultured at 30 °C in A1 medium (per liter of seawater: 10 g of starch, 4 g of yeast extract, 2 g of peptone, 10 mM Tris, pH 7.5; plus 18 g of agar for solid media). Spores were collected from 10 d liquid cultures at 5000 × *g* through a cotton wool packed sterile syringe. For genomic DNA preparation, *S. tropica* mycelia were lysed in 2% Triton X-100, 1% SDS, 100 mM sodium chloride, 1 mM EDTA, 10 mM Tris, pH 8.0, by vortexing with acid-washed glass beads. Genomic DNA was obtained by phenol/chloroform extraction, and residual RNA was digested with DNase-free RNase.

Gene Deletions in S. tropica CNB-440—Escherichia coli EPI300 cells with pCC1FOS-based fosmids harboring *strop0634* or *strop1447* were gifts from Bradley Moore. Apramycin and kanamycin resistance cassettes were amplified from plasmids pIJ773 and pIJ776 provided by Bertolt Gust using primer pairs with extensions homologous to 50-nt upstream and downstream of the *strop634* and *strop1447* start and stop codons. For disruption of the Strop634 ArsC domain, the 5′ primer was homologous to 50 nt of the linker

* This work was supported by Deutsche Forschungsgemeinschaft Grant Be2253/3 (to E. B.).
[S] The on-line version of this article (available at http://www.jbc.org) contains supplemental Figs. S1–S6.
[1] Both authors contributed equally to this work.
[2] To whom correspondence should be addressed: Pharmaceutical Institute, University of Kiel, Gutenbergstrasse 76, 24118 Kiel, Germany. Fax: 49-431-1352; E-mail: ebeitz@pharmazie.uni-kiel.de.

region. The primer further encoded a stop codon eventually yielding a truncated Strop634 protein. Homologous recombination was done in *E. coli* EPI300 using the Red/ET homology recombination kit (provided by Youming Zhang, GENEBridge) (16). Recombination was verified by PCR and sequencing of the junctions between the disruption cassettes and the fosmids. The fosmids were transferred by conjugation of the *E. coli* S17–1 mobilization strain (gift from Andreas Schlüter) (17) and *S. tropica* facilitated by *oriT* (RK2) sequences in the disruption cassettes (18). Resistant *S. tropica* colonies were restreaked on selective media four to five times before they were grown on nonselective medium. Gene targeting was verified by genomic PCR (supplemental Fig. S2).

S. tropica Membrane Protein Preparation and Western Blot—*S. tropica* cells were lysed in 10 mM magnesium chloride, 1 mM EDTA, 5% glycerol, 1 mM DTT, 1 mM PMSF, 20 mM Tris, pH 8.0, using a French pressure cell. The lysate was cleared by low speed centrifugation and the plasma membranes were collected at 100,000 × *g*. The pellet was resuspended and membrane proteins were precipitated by addition of 5% trichloroacetic acid for later use in Western blots. Polyclonal rabbit antisera were raised against heterologously expressed Strop634 and Strop1447 ArsC domains (Biogenes) and were affinity purified using columns with immobilized antigen.

Yeast Mutants and Complementation Assays—The BY4742 mother strain and the single deletions strains Δ*fps1* and Δ*acr2* were obtained from Euroscarf. BY4742 Δ*acr2,3* and Δ*acr2,3* Δ*fps1* were generated by replacing in the BY4742 and Δ*fps1* strains the chromosomal *acr2* and *acr3* region (1858 bp) with the LEU2 marker (from plasmid pGADT7, Clontech) using a one-step PCR approach (19). BY4742 Δ*acr2,3* Δ*fps1* was used to generate BY4742 Δ*acr2,3* Δ*fps1* Δ*ycf1* by replacing the *ycf1* open reading frame (4548 bp) by the HIS3 selection marker (from plasmid pEG202, Origene Technologies) flanked by sequences homologous to 1 kb upstream and downstream of *ycf1*. Gene replacement was confirmed by PCR. Genotypes and phenotypes in the presence of arsenate or arsenite are shown in supplemental Fig. S3. For growth complementation assays, the open reading frames of *Saccharomyces cerevisiae fps1*, *S. tropica strop634*, and *strop1447*, and *M. tuberculosis* H37Rv *Rv2643* were amplified from genomic DNA (H37Rv DNA was provided by Stefan Niemann), subcloned into pRS426Met, and the above yeast strains were transformed. Serial 10-fold dilutions of normalized cell suspensions were spotted on selective agar medium (SD-Ura) supplemented with arsenate or arsenite as indicated. Phenotypes were monitored after 3–5 days.

Direct Arsenite Permeability Assays—BY4742 Δ*acr2,3* Δ*fps1* Δ*ycf1* yeast cells expressing Fps1, Strop634, or Strop1447 from pRS426Met, as well as mock-transformed cells were grown in 50 ml of selective liquid medium (SD-Ura) to an A_{600} of 1.3. The cells were collected, resuspended in fresh medium to an A_{600} of 10, and exposed to 1 mM arsenite. Samples were taken in 10-min intervals and rapidly washed three times with ice-cold water. The cell pellets were dissolved in 65% nitric acid at 70 °C for 20 min for measurement of the intracellular arsenic content using a hydride generation atomic absorption spectrometer (3030B, PerkinElmer Life Sciences). The assays were done in triplicate using independently grown yeast cultures.

Direct Water and Glycerol Permeability Assays—Protoplasts of BY4742 Δ*fps1* yeast expressing Strop634, Strop1447, or PfAQP were prepared from 20 ml overnight cultures (SD-Ura). The cells were collected at 3000 × *g* and preincubated in 3 ml of equilibration buffer (50 mM potassium phosphate, 0.2% β-mercaptoethanol, pH 7.2) at 30 °C for 15 min. Then, 6 ml of digestion buffer (50 mM potassium phosphate, 2.4 M sucrose, 0.2% β-mercaptoethanol, 16.7 mg ml^{-1} bovine serum albumin, 0.33 mg ml^{-1} zymolyase 20T, pH 7.2) was added for incubation at 30 °C for 1 h. Protoplasts were collected at 3000 × *g*, washed once with 5 ml of incubation buffer (1.2 M sucrose, 50 mM sodium chloride, 5 mM calcium chloride, 10 mM Tris, pH 7) and resuspended in incubation buffer to an A_{600} of 2. For assaying, the protoplasts were rapidly mixed with an equal volume of mixing buffer (incubation buffer plus 0.6 M glycerol) at 15 °C in a stopped flow apparatus (SFM-300, BioLogic), and cell volume changes were monitored by measuring the intensity of 90° light scattering at 546 nm. In a first phase, cell volume decreased due to rapid water release according to the 300 mosmol kg^{-1} outward directed osmotic gradient leading to an increase in light scattering. In a second, slower phase, partial recovery of the cell volume indicated expression of functional aquaglyceroporins due to glycerol uptake driven by the 300 mM chemical gradient. The osmotic water permeability coefficient P_f was calculated using the following equation (20),

$$P_f = \frac{1}{\tau} \times \frac{V_0}{S_0 \times V_W \times C_{diff}} \quad \text{(Eq. 1)}$$

where τ is the time constant of the exponential fitting function, V_0 the initial mean protoplast volume (65.45 μm^3), S_0 is the initial mean protoplast surface area (78.54 μm^2), V_W is the partial molar water volume (18 cm^3 mol^{-1}), and C_{diff} is the concentration of the osmotically active solute after mixing (0.3 M or 3 × 10^{-4} mol cm^{-3}). The glycerol permeability coefficient P_{gly} was calculated from the second phase of the curve using the following equation (21),

$$P_{gly} = |dI/dt| \times \frac{V_0 \times C_{out}}{S_0 \times C_{diff}} \quad \text{(Eq. 2)}$$

where dI/dt is the initial slope of the light scattering intensity curve, V_0 and S_0 are as above, C_{out} is the total external solute concentration (1.5 M), and C_{diff} is the chemical glycerol gradient (0.3 M).

In Vitro Characterization of Strop634 and Strop1447 Arsenate Reductase Domains—DNA coding for the Strop634 and Strop1447 ArsC domains was amplified from genomic *S. tropica* DNA and subcloned into pQE30 (Qiagen) for expression in *E. coli* BL21 DE3 (pLysS) cells and affinity purification via an N-terminal His_6 tag. Arsenate reductase activity (0.25 μM of the purified enzyme domains plus 0–400 mM arsenate) was assayed photometrically in the presence of 6.72 μM *E. coli* thioredoxin, 0.345 μM *E. coli* thioredoxin reductase (both from Sigma), and 125 μM NADPH in 150 mM sodium

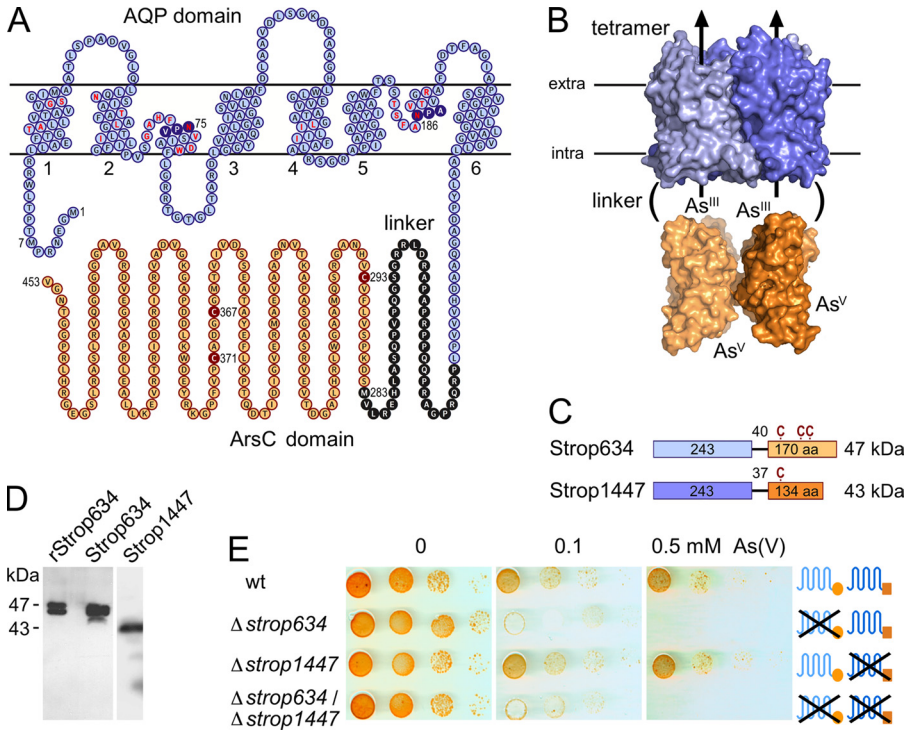

FIGURE 1. **A channel-enzyme fusion protein, Strop634, confers arsenate resistance in *S. tropica*.** *A*, topology prediction of Strop634. Labeled are the Asn-Pro-Ala (*NPA*) signature motifs (*filled blue circles*), putative residues of the channel interior (*red letters*), the ArsC domain start (position 283), and the catalytic cysteines (*filled red circles*). The plot was generated using TeXtopo (22). *B*, structure model of Strop634 and Strop1447 depicting the size relation of the channel and ArsC domains based on the *E. coli* aquaglyceroporin (Protein Data Bank code 1FX8) and ArsC (Protein Data Bank code 1J9B). *C*, domain arrangement of Strop634 and Strop1447, the latter carrying a single cysteine. The relative positions of the cysteines (*C*) are labeled above the *bars*. *D*, Western blot showing full-length expression of recombinant Strop634 in yeast (*rStrop634*), as well as Strop634 and Strop1447 in *S. tropica* using specific antisera directed against either reductase domain. *E*, arsenate sensitivity of *S. tropica* WT and deletion strains. 10-fold serial dilutions of *S. tropica* spores were spotted on agar medium containing 0, 0.1, or 0.5 mM arsenate and were incubated at 29 °C for 5 days.

chloride, 20 mM Tris, pH 7.5 (NADPH, $\epsilon_{340} = 6200\ M^{-1}\ cm^{-1}$). Phosphotyrosine phosphatase activity (10 μM of the purified enzyme domains plus 0–20 mM 4-nitrophenyl phosphate) was assayed in 150 mM sodium chloride, 20 mM Tris, pH 7.5 (nitrophenol, $\epsilon_{405} = 18{,}000\ M^{-1}\ cm^{-1}$).

RESULTS

A Single Gene, strop634, Confers Arsenate Resistance in S. tropica—The *S. tropica* genome (14) encodes Strop634 and Strop1447 (Fig. 1, *A–C*) as the only proteins putatively associated with arsenate detoxification. Their protein layout is unprecedented because it comprises two domains, *i.e.* an aquaglyceroporin-derived N-terminal channel-like part fused to a C-terminal enzyme domain with similarity to ArsC arsenate reductases. The channel domain is predicted to ~25 Å in diameter providing sufficient space for attached ArsC domains when oriented longitudinally (see model based on the respective *E. coli* aquaglyceroporin GlpF (23) and ArsC (24) structures) (Fig. 1*B*). Strop634 and Strop1447 share 81% sequence identity in the channel domain and 66% in the ArsC domain; the linker regions are unrelated. In the Strop634 linker, Met-283 marks the start of the ArsC domain (Fig. 1*A*), whereas in Strop1447, no such methionine is present (supplemental Fig. S1). Specific antisera generated against either ArsC domain detected the full-length fusion proteins of 47 and 43 kDa in *S. tropica* (Fig. 1*D* in comparison with recombinant Strop634). The double bands presumably derive from alternative translation starts at Met-1 and Met-7 (Fig. 1*A*). To assess the functionality in arsenate detoxification, we generated *S. tropica* deletion strains by disrupting *strop634* and *strop1447*. Lack of Strop634 rendered the single and double deletion strains highly sensitive to arsenate exposure, whereas in the absence of Strop1447, the cells unexpectedly displayed a normal resistance level (Fig. 1*D*). This led us to analyze the Strop634 and Strop1447 channel and ArsC domains in yeast model systems.

Functional Analysis of Channel and Reductase Domains in Yeast—S. cerevisiae expresses a single arsenate reductase, ACR2 (yeast type arsenate reductase). Deletion of the *acr2* gene yields an arsenate sensitive strain (Fig. 2*A*) (25). Heterologous expression of Strop634 or its separate ArsC domain complemented the *acr2* deletion and permitted cell growth comparable to the ACR2 control (Fig. 2*A*). The Strop1447 ArsC domain was nonfunctional. We then tested the channel domains of Strop634 and Strop1447 for arsenite permeability in a yeast strain lacking both endogenous arsenite transport proteins of the plasma membrane, ACR3 (26) and the aquaglyceroporin Fps1 (10). Due to the absence of an uptake pathway, this strain is fairly resistant to extracellular arsenite (Fig. 2*B*). Expression of Strop634 or its channel domain alone allowed arsenite to enter the cells and inhibited growth. Expression of the channel domain alone appeared somewhat less efficient, which might be related to suboptimal intracellular

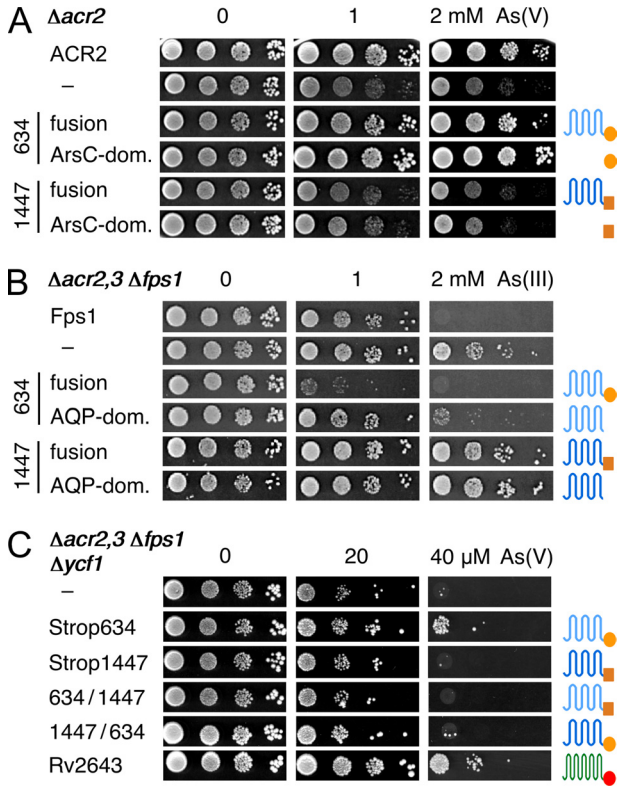

FIGURE 2. **Functional assessment of Strop634, Strop1447, and Rv2643 in yeast deletion strains.** *A*, complementation of Δ*acr2* yeast by expression of Strop634, Strop1447, and their separate ArsC domains (*dom.*). Cells were spotted on 0, 1, and 2 mM arsenate media and incubated at 29 °C for 4 days. *B*, assay for inward arsenite permeability. Expression of functional arsenite channels in Δ*acr2,3* Δ*fps1* yeast leads to reduced growth on 1 and 2 mM arsenite media. *C*, complementation of a highly arsenate sensitive yeast strain (Δ*acr2,3* Δ*fps1* Δ*ycf1*). Yeast growth indicates both reduction of arsenate and outward arsenite permeability. Cells expressing Strop634, Strop1447, Rv2643, and Strop chimeras with swapped channel and reductase domains were spotted on 0, 20, and 40 μM arsenate media.

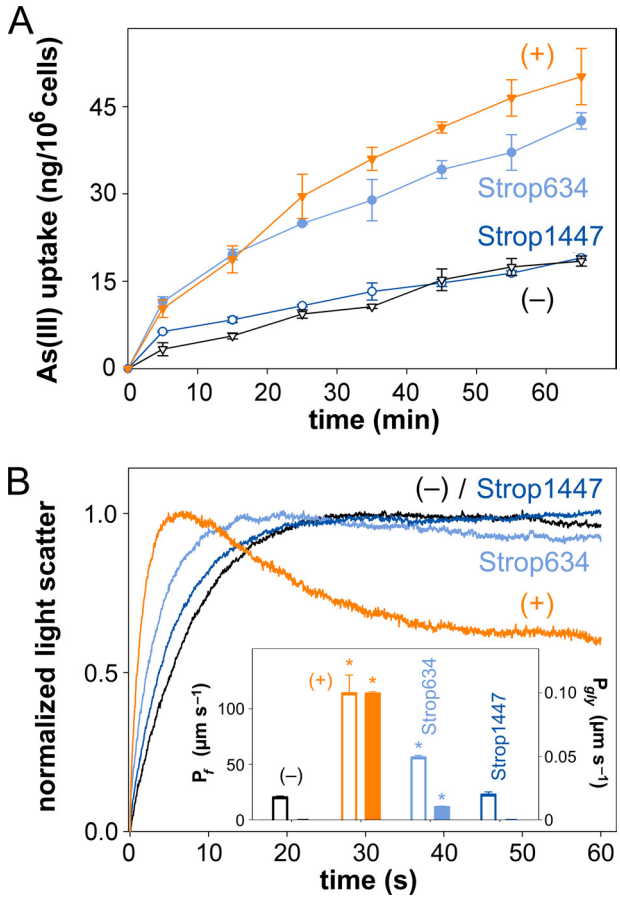

FIGURE 3. **Direct arsenite, water, and glycerol permeability assays.** *A*, shown is the accumulation of arsenic in 1 mM arsenite-exposed Δ*acr2,3* Δ*fps1* Δ*ycf1* yeast cells expressing Fps1 (+ control; *orange triangles*), Strop634 (*light blue circles*), Strop1447 (*dark blue circles*), or in nonexpressing cells (− control; *black triangles*). The *error bars* denote S.E. ($n = 3$). *B*, dynamic light scattering in a hyperosmotic, inward directed 300 mM glycerol gradient of Δ*fps1* yeast protoplasts expressing PfAQP (+ control; *orange trace*), Strop634 (*light blue trace*), Strop1447 (*dark blue trace*), or of nonexpressing protoplasts (− control; *black trace*). The first phase indicates osmotic water release, and the second phase indicates glycerol uptake. 10 traces were averaged per experiment. The insert shows water (P_f; *open bars*; *left* ordinate) and glycerol permeability coefficients (P_{gly}; *filled bars*; *right* ordinate) calculated from the traces. The *error bars* denote S.E. ($n = 10$). *Asterisks* label values that are significant ($p < 0.5$) compared with the − control.

trafficking or protein folding/stability of the truncated Strop634. Strop1447, again, was nonfunctional. We then asked whether a single yet dual functional protein could rescue a yeast strain that is highly sensitive to arsenate due to deletion of the ACR2 reductase and all transport proteins for arsenite, ACR3, Fps1, and the vacuolar ABC transporter Ycf1 for arsenite-thiol conjugates (Fig. 2*C*) (27). Strop634 and the ACR3-ArsC fusion protein Rv2643 from *M. tuberculosis* were able to detoxify arsenate, whereas Strop1447 and two chimeras with Strop634 carrying either the Strop1447 channel or ArsC domain were not (Fig. 2*C*). These phenotypic assays thus showed that both domains of Strop1447 are nonfunctional in the yeast system, whereas Strop634 constitutes a functional assembly of an arsenite channel and an ArsC.

Direct Transport Assays Confirm Arsenite Permeability of Strop634—To get a more quantitative and direct measure of the arsenite permeability we exposed Δ*acr2,3* Δ*fps1* Δ*ycf1* yeast cells expressing Strop634, Strop1447, or the endogenous Fps1 to 1 mM arsenite and determined the accumulation of intracellular arsenic over time by atomic absorption spectroscopy. The obtained data were in line with the phenotypic assays. Strop634 conducted arsenite at about the same rate as Fps1 (10) yielding 40 ng of intracellular arsenic per 10^6 cells within 1 h, whereas Strop1447 did not increase arsenite uptake over that of control cells lacking arsenite uptake pathways (Fig. 3*A*).

Strop634 Channel Domain Has Enhanced Selectivity for Arsenite and Low Glycerol Permeability—Considering sequence similarity, presence of Asn-Pro-Ala signature motifs, and a predicted six-transmembrane topology with two half-helices, the channel domains of Strop634 and Strop1447 are clearly aquaglyceroporin-derived (Fig. 1*A*). To test for water and glycerol permeability of Strop634 and Strop1447 in a direct assay, we monitored dynamic light scattering in a rapid mixing device after subjection of yeast protoplasts expressing Strop634, Strop1447, or the bifunctional *Plasmodium falciparum* water/glycerol channel, PfAQP (28), to a hyperosmotic glycerol gradient of 300 mM. In a first phase, due to hypertonic conditions, the protoplasts rapidly released water and shrank leading to an increase in light scattering. In a second phase, slower glycerol influx reduced the degree of light scat-

tering when functional aquaglyceroporins were present in the protoplasts (Fig. 3*B*). Accordingly, PfAQP expression led to an increase in the light scattering signal that was more than five times faster than that of the nonexpressing control protoplasts followed by a substantial recovery of the cell volume due to glycerol influx, whereas the control protoplasts lacked glycerol permeability. Resulting water and glycerol permeability coefficients are shown in the insert of Fig. 3*B*. Strop634 conducted water at half the rate of PfAQP (55 μm s^{-1} *versus* 113 μm s^{-1}) indicating general functionality of the channel. Yet, we found only very low Strop634 glycerol permeability (0.01 μm s^{-1}), which was one order of magnitude lower than that of PfAQP (0.1 μm s^{-1}) (Fig. 3*B*). We did not detect significant water or glycerol permeability of Strop1447.

In accordance with these direct assays, PfAQP expression complemented a Δ*fps1* yeast deletion strain in two types of phenotypic glycerol transport assays, whereas neither expression of Strop634 nor of Strop1447 affected the deletion phenotype (supplemental Fig. S4A) (29). The change in the selectivity bias of Strop634 against glycerol and for arsenite came as quite a surprise because aquaglyceroporins typically cannot discriminate between glycerol and arsenite and show permeability for both solutes (30). Inspection of the putative pore-lining amino acids of Strop634 (*red letters* in Fig. 1*A*; identical in Strop1447) as deduced from a structure model based on the crystal structures of the aquaglyceroporins from *E. coli*, GlpF (23), and *P. falciparum*, PfAQP (31), revealed notable differences. As common for all classical aquaglyceroporins, the interior of GlpF and PfAQP is amphipathic with only 18% polar amino acids located along one side of the channel wall. Yet, in Strop634, an unusual 39% of the channel forming residues are polar and provide hydrogen bonding sites around the pore perimeter. The region of the Strop634 channel corresponding to the aromatic/arginine selectivity filter of classical aquaglyceroporins (30) appears particularly hydrophilic with Asn-51 and Ser-183 replacing two conserved aromatic residues (supplemental Fig. S4, *B* and *C*). This may favor coordination of an arsenite molecule with a radial arrangement of hydroxyl groups over an amphipathic glycerol with all hydroxyl moieties pointing into the same direction. Currently, we are investigating which residues impair Strop1447 water/glycerol/arsenite permeability.

Strop634 ArsC Domain but Not That of Strop1447 Uses Thioredoxin as a Cofactor—The ArsC domains of Strop634 and Strop1447 show highest similarity to the low molecular weight phosphotyrosine phosphatase-derived type of arsenate reductase (5). These enzymes use thioredoxin as a cofactor that interacts with a catalytic thiol cascade formed by three conserved cysteine residues (5). All three cysteines are present in Strop634, whereas Strop1447 carries a single cysteine (Fig. 1, *A* and *C*). For *in vitro* characterization, we heterologously expressed the ArsC domains of Strop634 and Strop1447 in *E. coli* and affinity purified the proteins via an N-terminal His_6 tag. The Strop634 ArsC domain yielded thioredoxin and thioredoxin reductase-dependent arsenate reductase activity with a typical K_m of 75 mM and a k_{cat} of 13 min^{-1} (32), whereas Strop1447 was nonfunctional under these conditions (Fig. 4). The reaction cascade was sensitive to arsenite inhibition with thioredoxin reductase being the main target (supplemental Fig. S5). We detected residual phosphotyrosine phosphatase activity of Strop634 but not of Strop1447 using 4-nitrophenyl phosphate (K_m = 6.3 mM; k_{cat} = 0.016 min^{-1}) as an artificial substrate (Fig. 4, *inset*).

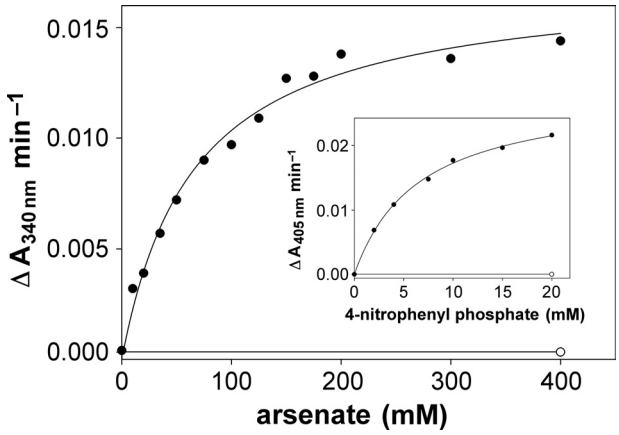

FIGURE 4. **In vitro analysis of Strop634 and Strop1447 ArsC activity.** The Michaelis-Menten plot shows the arsenate-dependent rate of NADPH oxidation by a mixture of Strop634 (*filled circles*) or Strop1447 (*open circle*) with thioredoxin and thioredoxin reductase. The insert depicts the rate of 4-nitrophenyl phosphate hydrolysis catalyzed by Strop634 (*filled circle*) and Strop1447 (*open circle*).

Hints for Activity of Strop1447 ArsC Domain in S. tropica—The lack of Strop1447 channel permeability and ArsC activity in phenotypic yeast assays and *in vitro* measurements posed the question whether *strop1447* is a translated yet nonfunctional pseudogene. Recently, two ArsC enzymes from *Corynebacterium glutamicum* were shown to couple to actinobacteria-specific mycothiol/mycoredoxin cofactors (32), which are analogous in function to glutathione/glutaredoxin of Gram-negative bacteria and eukaryotes. Their protein sequences are unrelated to Strop1447 but also carry a single cysteine, which suffices for catalysis. Various strains of the *Salinispora* genus have been shown to produce mycothiol (33) and respective putative genes for mycothiol biosynthesis (*mshA*, *strop331*; *mshB*, *strop3763*; *mshC*, *strop2168*; and *mshD*, *strop291*) and mycothiol reduction (*strop3319*) as well as for the mycoredoxin cofactor (*strop3740*) are present in the *S. tropica* genome (14). Coupling of Strop1447 to the mycothiol/mycoredoxin system would explain why we failed to detect Strop1447 ArsC activity in yeast and *in vitro* where mycothiol was absent. To obtain evidence for Strop1447 ArsC domain functionality in the physiological environment of the *S. tropica* cytosol, we generated a strain with a truncated *strop634* gene coding for the functional arsenite channel but lacking the ArsC domain. Respective cells would express Strop1447 as the only potential arsenate reductase, yet with a nonfunctional channel domain (see Figs. 2 and 3*A*). The resulting Δ*strop634-arsC* domain strain exhibited arsenate resistance, though somewhat weaker than wild-type *S. tropica* (Fig. 5*A*). This phenotype can be explained by an intermolecular mechanism of mycothiol-dependent arsenate reduction by Strop1447 and arsenite release via the Strop634 channel. Due to high sequence similarity in the channel domain, it is quite likely that the Strop634-Strop1447 protein interface is compatible per-

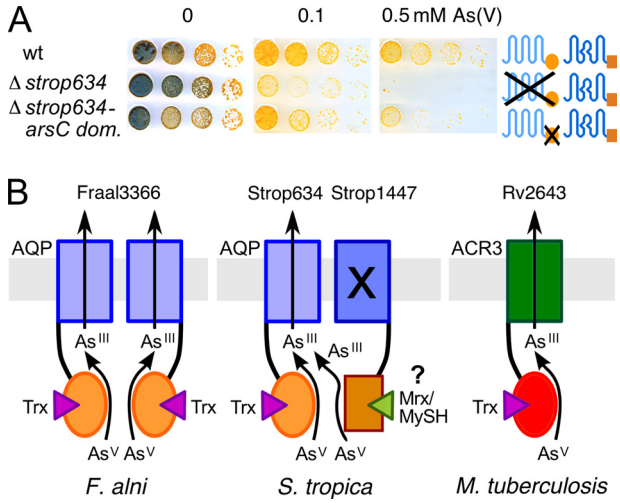

FIGURE 5. **Evidence for Strop1447 function in *S. tropica* arsenate resistance and models of channel enzyme functionality.** *A*, *S. tropica* WT as well as strains with full deletion of *strop634* or a partial deletion of the *strop634* ArsC domain (*dom.*) were spotted on arsenate media. The *strop1447* gene was left intact. *B*, derived models of dual-functional proteins in arsenate resistance using thioredoxin (*Trx*) or putatively mycoredoxin/mycothiol (*Mrx/MySH*).

mitting heterotetramer formation. Because ArsC enzymes have a low turnover (Fig. 4) (32), the presence of only two functional channels in a tetramer should suffice for unhindered export. However, at this stage we cannot fully exclude that a Strop634 and Strop1447 independent as yet unidentified arsenate reductase activity is located in the *S. tropica* cytosol. *In vitro* characterization of Strop1447 with regard to potential mycothiol-dependent arsenate reductase activity requires affinity purification of mycothiol from bacterial extracts and functional expression and purification of mycoredoxin and mycothiol reductase and has to await future studies. Furthermore, it will be tempting to investigate whether, by mutation, ArsC cofactor selectivity can be switched from thioredoxin to the alternative mycoredoxin pool (supplemental Fig. S1).

DISCUSSION

Aquaporins are ancient channel molecules that originated from a gene duplication event as evidenced by the prominent internal protein symmetry (23). Molecular variations in the selectivity filter region led to the functional separation of water specific, orthodox aquaporins from aquaglyceroporins conducting a wider spectrum of small, uncharged permeants, such as ammonia, urea, and glycerol (34). Aquaglyceroporins further constitute uptake pathways for trivalent arsenic in bacteria, yeast, and humans (1, 10, 11) and are, thus, mainly of toxicological interest. Recent evidence further assigns a role in arsenic detoxification to an aquaglyceroporin (12). The channel enzyme fusion proteins described in this study have reached a novel peak in evolution by assembling channels with optimized arsenite selectivity and arsenite-generating ArsC domains into one structure. Deduced schematic models of actinobacterial arsenate detoxifying fusion proteins are shown in Fig. 5*B*.

The fact that even closely related species of the *Frankia* genus (13) encode Strop634-like channel and enzyme domains in a fusion gene (*F. alni*; Fraal3366) as well as in two consecutive genes (*Frankia* sp. CcI3; Francci3_2325 and -2326) hints at recent evolutional fusion events. Furthermore, different types of arsenite exporters are encoded in the genomes of the closely related *Salinispora* species *S. tropica* (aquaglyceroporin-derived; Strop634) and *Salinispora arenicola* (ArsB; Sare2083) (35). This suggests recent lateral transfer of *strop634* homologues after the evolutional separation of the *S. tropica* and *S. arenicola* species. This conclusion is fostered by the location of clustered genes encoding channel and ArsC proteins with high similarity to Strop634 on an *Arthrobacter aurescens* TC1 plasmid (*pTC20056* & *20058*; supplemental Fig. S6) (36).

Metabolism generally depends on a dynamic equilibrium, which is maintained by enzymatic conversion and compartmentalization of intermediates. Immediate elimination of a metabolite from a reaction by transmembrane transport via channel enzyme fusion proteins would appear optimal. ArsC proteins seem predestined for fusions due to their small size and, indeed, other examples of fusions between a solute channel and a respective metabolic enzyme remain to be identified. Yet, in signal transduction, certain proteins depict a similar domain arrangement, *i.e.* a cation channel domain fused with an ADP ribase (TRPM2) (37), a kinase (TRPM7) (38), or an adenylyl cyclase (found in protozoa) (39); they are, however, of unrelated, probably sensory function. Transmembrane transport by facilitated diffusion is an energy-efficient process solely driven by the chemical gradient. The fusion of a metabolic enzyme to a corresponding substrate channel should improve efficiency in mainly two respects: in-place generation of the permeant by channel enzymes (i) increases the local metabolite concentration and hence directly couples the reaction enthalpy to the extrusion process (40) and (ii) prevents toxic cellular accumulation of metabolites.

Acknowledgments—We thank B. Moore for providing S. tropica fosmids, B. Gust for apramycin and kanamycin resistance cassettes, Y. Zhang for the Red/ET homology recombination system, A. Schlüter for the E. coli S17–1 mobilization strain, S. Niemann for M. tuberculosis H37Rv genomic DNA, and B. Henke for technical assistance.

REFERENCES

1. Oremland, R. S., and Stolz, J. F. (2003) *Science* **300,** 939–944
2. Turner, A. W. (1949) *Nature* **164,** 76–77
3. Luecke, H., and Quiocho, F. A. (1990) *Nature* **347,** 402–406
4. Moore, S. A., Moennich, D. M., and Gresser, M. J. (1983) *J. Biol. Chem.* **258,** 6266–6271
5. Messens, J., and Silver, S. (2006) *J. Mol. Biol.* **362,** 1–17
6. Adamson, S. R., and Stevenson, K. J. (1981) *Biochemistry* **20,** 3418–3424
7. Luthman, M., and Holmgren, A. (1982) *Biochemistry* **21,** 6628–6633
8. Tapio, S., and Grosche, B. (2006) *Mutat. Res.* **612,** 215–246
9. Achour, A. R., Bauda, P., and Billard, P. (2007) *Res. Microbiol.* **158,** 128–137
10. Wysocki, R., Chéry, C. C., Wawrzycka, D., Van Hulle, M., Cornelis, R., Thevelein, J. M., and Tamás, M. J. (2001) *Mol. Microbiol.* **40,** 1391–1401
11. Liu, Z., Shen, J., Carbrey, J. M., Mukhopadhyay, R., Agre, P., and Rosen, B. P. (2002) *Proc. Natl. Acad. Sci. U.S.A.* **99,** 6053–6058
12. Yang, H. C., Cheng, J., Finan, T. M., Rosen, B. P., and Bhattacharjee, H. (2005) *J. Bacteriol.* **187,** 6991–6997
13. Normand, P., Lapierre, P., Tisa, L. S., Gogarten, J. P., Alloisio, N., Bagn-

arol, E., Bassi, C. A., Berry, A. M., Bickhart, D. M., Choisne, N., Couloux, A., Cournoyer, B., Cruveiller, S., Daubin, V., Demange, N., Francino, M. P., Goltsman, E., Huang, Y., Kopp, O. R., Labarre, L., Lapidus, A., Lavire, C., Marechal, J., Martinez, M., Mastronunzio, J. E., Mullin, B. C., Niemann, J., Pujic, P., Rawnsley, T., Rouy, Z., Schenowitz, C., Sellstedt, A., Tavares, F., Tomkins, J. P., Vallenet, D., Valverde, C., Wall, L. G., Wang, Y., Medigue, C., and Benson, D. R. (2007) *Genome Res.* **17,** 7–15

14. Udwary, D. W., Zeigler, L., Asolkar, R. N., Singan, V., Lapidus, A., Fenical, W., Jensen, P. R., and Moore, B. S. (2007) *Proc. Natl. Acad. Sci. U.S.A.* **104,** 10376–10381
15. Cole, S. T., Brosch, R., Parkhill, J., Garnier, T., Churcher, C., Harris, D., Gordon, S. V., Eiglmeier, K., Gas, S., Barry, C. E., 3rd, Tekaia, F., Badcock, K., Basham, D., Brown, D., Chillingworth, T., Connor, R., Davies, R., Devlin, K., Feltwell, T., Gentles, S., Hamlin, N., Holroyd, S., Hornsby, T., Jagels, K., Krogh, A., McLean, J., Moule, S., Murphy, L., Oliver, K., Osborne, J., Quail, M. A., Rajandream, M. A., Rogers, J., Rutter, S., Seeger, K., Skelton, J., Squares, R., Squares, S., Sulston, J. E., Taylor, K., Whitehead, S., and Barrell, B. G. (1998) *Nature* **393,** 537–544
16. Zhang, Y., Buchholz, F., Muyrers, J. P., and Stewart, A. F. (1998) *Nat. Genet.* **20,** 123–128
17. Schäfer, A., Kalinowski, J., Simon, R., Seep-Feldhaus, A. H., and Pühler, A. (1990) *J. Bacteriol.* **172,** 1663–1666
18. Gust, B., Challis, G. L., Fowler, K., Kieser, T., and Chater, K. F. (2003) *Proc. Natl. Acad. Sci. U.S.A.* **100,** 1541–1546
19. Brachmann, C. B., Davies, A., Cost, G. J., Caputo, E., Li, J., Hieter, P., and Boeke, J. D. (1998) *Yeast* **14,** 115–132
20. Bertl, A., and Kaldenhoff, R. (2007) *FEBS Lett.* **581,** 5413–5417
21. Beitz, E., Wu, B., Holm, L. M., Schultz, J. E., and Zeuthen, T. (2006) *Proc. Natl. Acad. Sci. U.S.A.* **103,** 269–274
22. Beitz, E. (2000) *Bioinformatics* **16,** 1050–1051
23. Fu, D., Libson, A., Miercke, L. J., Weitzman, C., Nollert, P., Krucinski, J., and Stroud, R. M. (2000) *Science* **290,** 481–486
24. Martin, P., DeMel, S., Shi, J., Gladysheva, T., Gatti, D. L., Rosen, B. P., and Edwards, B. F. (2001) *Structure* **9,** 1071–1081
25. Mukhopadhyay, R., and Rosen, B. P. (1998) *FEMS Microbiol. Lett.* **168,** 127–136
26. Wysocki, R., Bobrowicz, P., and Ułaszewski, S. (1997) *J. Biol. Chem.* **272,** 30061–30066
27. Ghosh, M., Shen, J., and Rosen, B. P. (1999) *Proc. Natl. Acad. Sci. U.S.A.* **96,** 5001–5006
28. Hansen, M., Kun, J. F., Schultz, J. E., and Beitz, E. (2002) *J. Biol. Chem.* **277,** 4874–4882
29. Uzcategui, N. L., Szallies, A., Pavlovic-Djuranovic, S., Palmada, M., Figarella, K., Boehmer, C., Lang, F., Beitz, E., and Duszenko, M. (2004) *J. Biol. Chem.* **279,** 42669–42676
30. Wu, B., and Beitz, E. (2007) *Cell Mol. Life Sci.* **64,** 2413–2421
31. Newby, Z. E., O'Connell, J., 3rd, Robles-Colmenares, Y., Khademi, S., Miercke, L. J., and Stroud, R. M. (2008) *Nat. Struct. Mol. Biol.* **15,** 619–625
32. Ordóñez, E., Van Belle, K., Roos, G., De Galan, S., Letek, M., Gil, J. A., Wyns, L., Mateos, L. M., and Messens, J. (2009) *J. Biol. Chem.* **284,** 15107–15116
33. Newton, G. L., Jensen, P. R., Macmillan, J. B., Fenical, W., and Fahey, R. C. (2008) *Arch. Microbiol.* **190,** 547–557
34. Wu, B., Steinbronn, C., Alsterfjord, M., Zeuthen, T., and Beitz, E. (2009) *EMBO J.* **28,** 2188–2194
35. Penn, K., Jenkins, C., Nett, M., Udwary, D. W., Gontang, E. A., McGlinchey, R. P., Foster, B., Lapidus, A., Podell, S., Allen, E. E., Moore, B. S., and Jensen, P. R. (2009) *ISME J.* **3,** 1193–1203
36. Mongodin, E. F., Shapir, N., Daugherty, S. C., DeBoy, R. T., Emerson, J. B., Shvartzbeyn, A., Radune, D., Vamathevan, J., Riggs, F., Grinberg, V., Khouri, H., Wackett, L. P., Nelson, K. E., and Sadowsky, M. J. (2006) *PLoS. Genet.* **2,** e214
37. Perraud, A. L., Fleig, A., Dunn, C. A., Bagley, L. A., Launay, P., Schmitz, C., Stokes, A. J., Zhu, Q., Bessman, M. J., Penner, R., Kinet, J. P., and Scharenberg, A. M. (2001) *Nature* **411,** 595–599
38. Runnels, L. W., Yue, L., and Clapham, D. E. (2001) *Science* **291,** 1043–1047
39. Weber, J. H., Vishnyakov, A., Hambach, K., Schultz, A., Schultz, J. E., and Linder, J. U. (2004) *Cell Signal.* **16,** 115–125
40. Mitchell, P. (1957) *Nature* **180,** 134–136